

The efficient computation of transition state resonances and reaction rates from a quantum normal form

Roman Schubert, Holger Waalkens, and Stephen Wiggins

School of Mathematics, University Walk, University of Bristol, Bristol BS8 1TW, United Kingdom

(Dated: July 15, 2018)

A quantum version of a recent formulation of transition state theory in *phase space* is presented. The theory developed provides an algorithm to compute quantum reaction rates and the associated Gamov-Siegert resonances with very high accuracy. The algorithm is especially efficient for multi-degree-of-freedom systems where other approaches are no longer feasible.

PACS numbers: 82.20.Ln, 34.10.+x, 05.45.-a

Introduction. — The question of how, as Marcus [1] formulates it, a system “skis the reaction slope” is one of the crucial questions in reaction dynamics. Experimental techniques like photodissociation of jet-cooled molecules, molecular beam experiments or transition state spectroscopy give detailed information about the reaction process as has recently been demonstrated, e.g., for the ‘paradigm’ reaction of Hydrogen atom-diatom collisions (see, e.g., the review paper [2]). A chemical reaction can often be viewed as the scattering problem across a saddle point of the interaction potential. The cumulative reaction probability is then given by

$$N(E) = \text{tr } \hat{t} \hat{t}^T = \sum_{n_R n_P} |\langle \psi_{\text{out } n_P} | \hat{S} | \psi_{\text{in } n_R} \rangle|^2 \quad (1)$$

where \hat{t} is the transmission subblock of the scattering operator \hat{S} for energy E and the summation in the latter expression runs over all incoming reactant states with quantum numbers n_r and outgoing product states with quantum numbers n_p . The *ab initio* quantum mechanical computation of $N(E)$ soon becomes very expensive if the number of atoms in the system increases beyond 3 and one has to resort to suitable approximations. The main approach to compute $N(E)$ *classically* is transition state theory which was invented by Eyring, Polanyi and Wigner in the 30’s. The main idea is to define a dividing surface that divides the energy surface into a reactant and a product component and compute the rate from the directional phase space flux through this surface. In order not to overestimate the rate the dividing surface must not be recrossed by reactive trajectories. In the 70’s Pechukas, Pollak and others [3] showed that for two degrees of freedom such a dividing surface can be constructed from a periodic orbit that leads to the so called *periodic orbit dividing surface*. Recently it has been shown that a generalization to higher dimension can be achieved from a *normally hyperbolic invariant manifold* (NHIM) [4] — a fundamentally new object that takes the place of the periodic orbit. The dynamics is controlled by the NHIM’s stable and unstable manifolds which act as separatrices that divide the reactive trajectories from the nonreactive trajectories. The NHIM, its

stable and unstable manifolds and a dividing surface with the desired properties can be directly constructed from an algorithm based on a Poincaré-Birkhoff normal form procedure [5].

Much effort has been devoted to developing a quantum version of transition state theory whose implementation remains feasible for multi-dimensional systems (see the flux-flux autocorrelation function formalism by Miller and coworkers [6]). In this Letter we present a quantum version of the normal form procedure that lead to the construction of the high-dimensional phase space structures that govern the classical reaction dynamics and demonstrate that this *quantum normal form* approach to transition state theory provides an efficient procedure to compute quantum reaction rates and the corresponding Gamov-Siegert resonances [7].

The quantum normal form. — The main idea of which the seed can already be found, e.g., in [8], is to derive a local approximation of the Hamilton operator of the scattering problem that is valid near the saddle, and in order to facilitate further computations, takes a much simpler form than the original Hamiltonian. This can be achieved in a systematic way by a procedure based on the Wigner-Weyl calculus that has been used by others before to compute energy spectra associated with stable equilibria [9]. Here the manipulations of an operator \hat{A} are expressed in terms of its *symbol* which is the function $A(p, x)$ on the f -degrees-of-freedom phase space $(p, x) \in \mathbb{R}^{2f}$ defined by

$$\hat{A}\psi(x) = \frac{1}{(2\pi\hbar)^f} \int_{\mathbb{R}^{2f}} e^{\frac{i}{\hbar}\langle x-y, p \rangle} A\left(p, \frac{x+y}{2}\right) \psi(y) dy dp. \quad (2)$$

Defining the multiplication $*$ of two symbols A and B according to

$$A * B = A \exp\left(\frac{\hbar}{2} [\langle \overleftarrow{\partial}_x, \overrightarrow{\partial}_p \rangle - \langle \overrightarrow{\partial}_x, \overleftarrow{\partial}_p \rangle]\right) B, \quad (3)$$

where the arrows indicate whether the partial differentiation acts to the left (on A) or to the right (on B), gives the property that the quantization of the product of two symbols A and B is equal to the product of the quantizations of the individual symbols, i.e. $\widehat{AB} = \widehat{A} * \widehat{B}$. The

*-product leads to the definition of the Moyal bracket

$$\{A, B\}_M = \frac{i}{\hbar}(A * B - B * A). \quad (4)$$

We define the *order* s of a monomial $p^\alpha x^\beta \hbar^n \equiv p_1^{\alpha_1} \cdots p_f^{\alpha_f} x_1^{\beta_1} \cdots x_f^{\beta_f} \hbar^n$ according to $s = |\alpha| + |\beta| + 2n \equiv \alpha_1 + \cdots + \alpha_f + \beta_1 + \cdots + \beta_f + 2n$, and denote the vector space of polynomials spanned by monomials of order s by \mathcal{W}^s . For $A \in \mathcal{W}^s$ and $B \in \mathcal{W}^{s'}$ we define the Moyal adjoint by $\text{Mad}_A B := \{A, B\}_M$, then its iterates satisfy $[\text{Mad}_A]^n B \in \mathcal{W}^{n(s-2)+s'}$.

We start from a Hamilton operator \hat{H} whose symbol has expansion

$$H = E_0 + \sum_{s=2}^{\infty} H_s \quad (5)$$

where E_0 is a constant energy and $H_s \in \mathcal{W}^s$. Like in the case of classical transition state theory [5] we assume that the second order term is of the form

$$H_2 = \lambda I + \omega_2 J_2 + \cdots + \omega_f J_f \quad (6)$$

with the integrals

$$I = p_1 x_1, \quad J_k = \frac{1}{2}(p_k^2 + x_k^2), \quad k = 2, \dots, f. \quad (7)$$

This corresponds to a classical equilibrium point of saddle-center-...-center stability type ('saddle' for short), i.e. the matrix associated with the linearized system has one pair of real eigenvalues $\pm\lambda$ associated with the saddle or 'reaction coordinate' and $f-1$ pairs of imaginary eigenvalues $\pm i\omega_k$, $k = 2, \dots, f$, associated with the center or 'bath' degrees of freedom. Note that $p_1 x_1 = (\tilde{p}_1^2 - \tilde{q}_1^2)/2$ where (p_1, x_1) and $(\tilde{p}_1, \tilde{q}_1)$ are related by a rotation of 45° . We restrict ourselves to the generic non-resonant case where the frequencies ω_k , $k = 2, \dots, f$, are rationally independent

In order to simplify the Hamiltonian \hat{H} we will transform it by successive conjugations with unitary operators, $\hat{H} =: \hat{H}^{(2)} \rightarrow \hat{H}^{(3)} \rightarrow \hat{H}^{(4)} \rightarrow \cdots \rightarrow \hat{H}^{(N)}$, where

$$\hat{H}^{(n)} = e^{i\hat{W}_n/\hbar} \hat{H}^{(n-1)} e^{-i\hat{W}_n/\hbar}, \quad (8)$$

with $W_n \in \mathcal{W}^n$. Using the Moyal adjoint the symbol of the right hand side can be expanded as

$$H^{(n)} = \sum_{k=0}^{\infty} \frac{1}{k!} [\text{Mad}_{W_n}]^k H^{(n-1)}. \quad (9)$$

If we expand furthermore each of the symbols $H^{(n)}$ in a generalized Taylor series as in (5), $H^{(n)} = E_0 + \sum_{s \geq 2} H_s^{(n)}$, with $H_s^{(n)} \in \mathcal{W}^s$, then using (9) the terms in these series can be related by

$$H_s^{(n)} = \sum_{k=0}^{\lfloor \frac{s-2}{2} \rfloor} \frac{1}{k!} [\text{Mad}_{W_n}]^k H_{s-n(k-2)}^{(n-1)}, \quad (10)$$

where $[\cdot]$ denotes the integer part. Notice that for $s < n$, $H_s^{(n)} = H_s^{(n-1)}$, and for $s = n$ we obtain

$$H_n^{(n)} = H_n^{(n-1)} + \{W_n, H_2\} \quad (11)$$

where we have used that $H_2^{(n)} = H_2$ for all $n \geq 3$ and that the Moyal bracket reduces to the Poisson bracket $\{\cdot, \cdot\}$ if one of the functions is quadratic. This is the homological equation which is familiar from the classical normal form algorithm, [5], and under the non-resonance conditions on the frequencies ω_k , given any $H_n^{(n-1)} \in \mathcal{W}^n$ there exists a unique $W_n \in \mathcal{W}^n$ such that $H_n^{(n)}$ can be written as a function of the actions I, J_2, \dots, J_f alone (or, equivalently, $H_n^{(n)}$ satisfies $\{I, H_n^{(n)}\} = \{J_2, H_n^{(n)}\} = \cdots = \{J_f, H_n^{(n)}\} = 0$).

Choosing the generators of the unitary transformations W_n recursively for $n = 3, 4, \dots, N$ as solutions of (11) we obtain an operator $\hat{H}^{(N)}$ whose symbol is of the form $H^{(N)} = E_0 + \sum_{s=2}^N H_s^{(N)} + R^{(N+1)}$ where the first part is a polynomial in the actions I, J_2, \dots, J_f , i.e., is in *normal form*, and the remainder $R^{(N+1)}$ consists of terms of order $N+1$ and higher. In a final step we want to express the quantization of the normal form part as an operator function of the quantized actions \hat{I} and \hat{J}_k . To this end we use a recursion relation for \hat{I}^n (and a similar one for the J_k), $\hat{I}^{n+1} = \hat{I}\hat{I}^n - \hat{I}^{n-1}n^2\hbar^2/4$, which can be derived from the product formula (3). This allows us to express quantizations of powers of I as a polynomial in powers of \hat{I} . In this way we find a polynomial $H_{\text{QNF}}^{(N)}$ such that

$$U_N^* \hat{H} U_N = H_{\text{QNF}}^{(N)}(\hat{I}, \hat{J}_2, \dots, \hat{J}_f) + \hat{R}^{(N+1)}, \quad (12)$$

where $U_N = \prod_{n=3}^N e^{-i\hat{W}_n/\hbar}$. $H_{\text{QNF}}^{(N)}(\hat{I}, \hat{J}_2, \dots, \hat{J}_f)$ is called the *quantum normal form* (QNF) of \hat{H} of order N . The remainder term $\hat{R}^{(N+1)}$ has a symbol which is of order $N+1$ and is therefore very small near the saddle point. Hence the dynamics near the saddle point can be described with high accuracy by the QNF Hamiltonian. The advantage of the QNF Hamiltonian is that it is an operator function of the commuting operators \hat{I} and \hat{J}_k whose properties are well understood. Finally we point out that in the limit $\hbar \rightarrow 0$ we recover the classical normal form of order N , $\lim_{\hbar \rightarrow 0} H_{\text{QNF}}^{(N)}(I, J_2, \dots, J_f) = H_{\text{cl}}^{(N)}$.

We implemented the algorithm of the QNF computation in the programming language C++.

Resonances and reaction rates.— The eigenfunctions of the truncated QNF Hamiltonian are tensor products of harmonic oscillator wave functions for the center degrees of freedom x_k , $k = 2, \dots, f$, and eigenfunctions of the operator

$$\hat{I} = \frac{\hbar}{i} \left(x_1 \partial_{x_1} + \frac{1}{2} \right) \quad (13)$$

associated with the saddle direction. The operator \hat{I} has

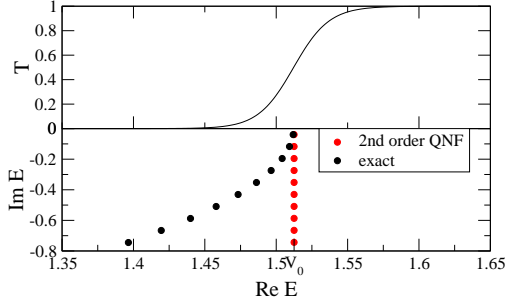


FIG. 1: Transmission probability $T(E)$ and Gamov-Siegert resonances in the complex energy plane for the Eckart potential. The parameters are $a = 1$, $10A = B = 5$ for the Eckart potential, and $m = 1$ and $\hbar = 0.1$.

eigenfunctions [10]

$$\psi_{\text{out} \pm}(x_1) = \Theta(\pm x_1) |x_1|^{-1/2 + iI/\hbar}, \quad (14)$$

Θ being the step function, which are outgoing waves. Incoming waves can be defined from the Fourier transforms

$$\psi_{\text{in} \pm}(x_1) = \frac{1}{\sqrt{2\pi\hbar}} \int \psi_{\text{out} \mp}^*(y_1) e^{\frac{i}{\hbar} x_1 y_1} dy_1. \quad (15)$$

Note that in order to classify the eigenfunctions as ‘outgoing’ or ‘incoming’ it is convenient to rotate the coordinates (p_1, x_1) back to the more standard notation $(\tilde{p}_1, \tilde{q}_1)$ for a potential barrier mentioned above. Expressing the functions $\psi_{\text{in} \pm}$ in terms of $\psi_{\text{out} \pm}$ gives the entries of a ‘local S-matrix’,

$$\psi_{\text{in} +} = S_{n11} \psi_{\text{out} +} + S_{n12} \psi_{\text{out} -}, \quad (16)$$

$$\psi_{\text{in} -} = S_{n21} \psi_{\text{out} +} + S_{n22} \psi_{\text{out} -}. \quad (17)$$

Here n denotes the vector of nonnegative integers (n_2, \dots, n_f) formed by the quantum numbers of the modes in the center directions. The local S-matrix is block diagonal due to the separability of the QNF. Mode mixing is a ‘global’ effect which occurs from connecting the local wave functions to the asymptotic reactants and products wave functions. However, the local S-matrix alone already contains the full information needed to compute reaction rates and resonances.

Evaluating the integrals (15) gives

$$S_n(E) = \frac{e^{i(\frac{\pi}{4} - \frac{I}{\hbar} \ln \hbar)}}{\sqrt{2\pi}} \Gamma\left(\frac{1}{2} - i\frac{I}{\hbar}\right) \begin{pmatrix} -ie^{-\frac{\pi}{2} \frac{I}{\hbar}} & e^{\frac{\pi}{2} \frac{I}{\hbar}} \\ e^{\frac{\pi}{2} \frac{I}{\hbar}} & -ie^{-\frac{\pi}{2} \frac{I}{\hbar}} \end{pmatrix} \quad (18)$$

with I being implicitly defined by

$$H_{\text{QNF}}^{(N)}(I, \hbar(n_2 + 1/2), \dots, \hbar(n_f + 1/2)) = E. \quad (19)$$

The transmission probability of mode n is

$$T_n(E) = |S_{n12}(E)|^2 = (1 + e^{-2\pi \frac{I}{\hbar}})^{-1}, \quad (20)$$

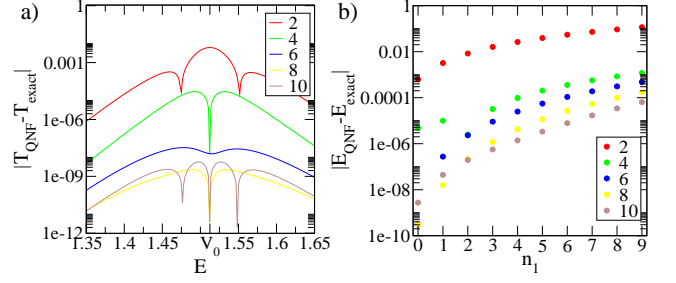


FIG. 2: (a) Errors for the transmission probability of the Eckart potential computed from the QNF. (b) Errors for the QNF resonances (differences between the corresponding QNF and exact complex energies) of the Eckart potential as a function of the quantum number n_1 . The different colors correspond to different orders of the QNF. The parameters for the Eckart potential are the same as in Fig. 1.

which gives the cumulative reaction probability $N(E) = \sum_n T_n(E)$. The S-matrix has poles at $I = -i\hbar(n_1 + 1/2)$ for nonnegative integers n_1 and these define the Gamov-Siegert resonances via (19).

Examples.— We at first illustrate the procedure for 1D potential barriers, i.e. Hamiltonians of the form $H = p^2/(2m) + V(x)$, where $V(x)$ has a maximum which we can assume to be at $x = 0$. The second order QNF is easily obtained and gives the well know result $\hat{H}_{\text{QNF},2} = V(0) + \lambda \hat{I}$ with $\lambda = (-V''(0)/m)^{1/2}$ which is equivalent to approximating the potential barrier by an inverted parabola. The first nontrivial correction to this result comes from the fourth order QNF $\hat{H}_{\text{QNF},4}$ given by

$$V(0) + \lambda \hat{I} + \frac{1}{16m^2\lambda^2} \left(\frac{5}{3m\lambda^2} V'''(0) + V^{IV}(0) \right) \hat{I}^2 - \frac{1}{64m^2\lambda^2} \left(\frac{7}{9m\lambda^2} V'''(0) + V^{IV}(0) \right) \hbar^2. \quad (21)$$

We apply the QNF to the Eckart potential [12]

$$V_{\text{Eckart}}(x) = A \frac{e^{(x+x_0)/a}}{1 + e^{(x+x_0)/a}} + B \frac{e^{(x+x_0)/a}}{(1 + e^{(x+x_0)/a})^2} \quad (22)$$

with $x_0 = a \ln(B+A)/(B-A)$ and $B > A \geq 0$. Figure 1 shows the exact transmission probability which is known analytically, and the exact string of resonances together with the resonances from the second order QNF which have constant imaginary part. The bending of the string of exact resonances is a nonlinear effect that is very well described already by the fourth order QNF. The excellent accuracy of the resonances and the cumulative reaction probability computed from higher orders of the QNF is illustrated in Fig. 2.

We next consider the two-degree-of-freedom example of a Hamiltonian with an Eckart potential in the x_1 -direction, a Morse potential

$$V_{\text{Morse}}(x_2) = D_e (e^{-2\alpha x_2} - 2e^{-\alpha x_2}) \quad (23)$$

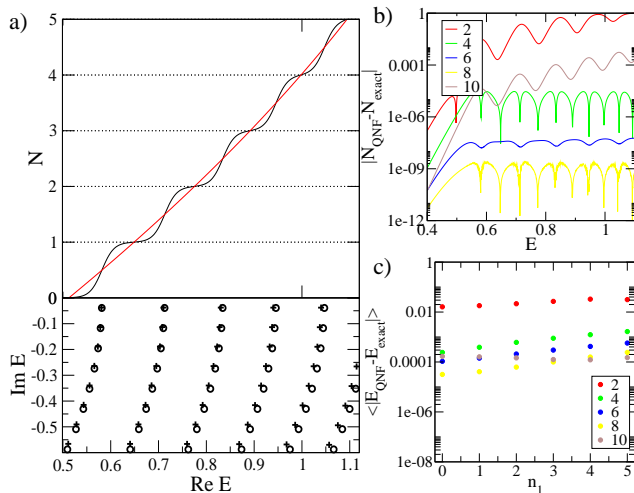


FIG. 3: (a) The top panel shows the cumulative reaction probability $N(E)$ (oscillatory curve) and the classical flux divided by $2\pi\hbar$ (smooth curve) for the Eckart-Morse potential defined in the text with $\epsilon = 0$. The bottom panel shows the resonances in the complex energy plane marked by circles for the uncoupled case $\epsilon = 0$ and by crosses for the strongly coupled case $\epsilon = 0.3$. For the coupled case the numerically exact resonances are computed from the complex dilation method [13]. The parameters for the Eckart potential are the same as in Fig. 1. The parameters for the Morse potential are $D_e = 1$ $\alpha = 1$. Again we choose $m = 1$ and $\hbar = 0.1$. (b) Errors for the cumulative reaction probability in (a) for different orders of the QNF. (c) Average errors $\langle |E_{\text{QNF}} - E_{\text{exact}}| \rangle_{n_1} = \sum_{n_2=0}^5 |E_{\text{QNF}}(n_1, n_2) - E_{\text{exact}}(n_1, n_2)|/6$ for the QNF resonances in (a) for the coupled case $\epsilon = 0.3$ as a function of the quantum numbers n_1 .

in the x_2 -direction, plus a kinetic coupling $\epsilon p_1 p_2$. In Fig. 3 the cumulative reaction probability and the resonances computed from the QNF are compared with the exact results. In the uncoupled case $\epsilon = 0$, $N(E)$ increases as a function of E at integer steps each time a new transition channel opens, i.e. when the transmission probability $T_{n_2}(E)$ of a Morse oscillator mode n_2 switches from 0 to 1. For both the uncoupled and strongly coupled case the resonances form a distorted lattice parametrized by the mode quantum number n_2 in horizontal direction and the quantum number n_1 in vertical direction. Similar to the 1D example, each string of constant n_2 is related to one step of $N(E)$.

Like in the 1D case the agreement of the QNF results with the exact results is excellent and this remains the case even for the strongly coupled system. The QNF is an asymptotic expansion which in general does not converge. For the system shown in the example this can be seen from the fact that the 10th order QNF does not lead to an improvement of the results obtained from the 8th order QNF.

Conclusions.— The QNF computation of reaction probabilities and the corresponding Gamov-Siegert resonances is highly promising since it opens the way to study high dimensional systems for which other techniques based on the *ab initio* solution of the quantum

scattering problem like the complex dilation method [13] or the utilization of an absorbing potential [14] are no longer feasible. In fact, the numerical effort for computing the QNF is only slightly higher than the effort for computing the classical normal form (NF). The main difference is that the Poisson bracket in the classical NF needs to be replaced by the Moyal bracket. The storage of the QNF polynomials also requires only a disk space similar to the classical NF. Moreover, the QNF gives an explicit formula for the resonances from which they can be computed directly by inserting the corresponding quantum numbers. This leads to a direct assignment of the resonances. The QNF provides a quantum version of transition state theory that, in the semiclassical limit, is in accord with the classical phase structures that govern the reaction dynamics. In fact, the classical phase space structures form the skeleton for the scattering and resonance wavefunctions, and exploiting this relationship which will give a deep insight into the now experimentally accessible quantum reaction dynamics is the subject of our future studies (see also [15]).

This work was supported by the Office of Naval Research, EPSRC and the Royal Society.

-
- [1] R. A. Marcus, *Science* **256**, 1523 (1992).
 - [2] R. T. Skodje and X. Yang, *Int. Rev. Phys. Chem.* **23**, 253 (2004).
 - [3] P. Pechukas and F. J. McLafferty, *J. Chem. Phys.* **58**, 1622 (1973); P. Pechukas and E. Pollak, *J. Chem. Phys.* **69**, 1218 (1978).
 - [4] S. Wiggins, *Physica D* **44**, 471 (1990); S. Wiggins, *Normally Hyperbolic Invariant Manifolds in Dynamical Systems* (Springer, Berlin, 1994); S. Wiggins, L. Wiesenfeld, C. Jaffé, and T. Uzer, *Phys. Rev. Lett.* **86**, 5478 (2001).
 - [5] T. Uzer, C. Jaffé, J. Palacián, P. Yanguas, and S. Wiggins, 957 (2001); H. Waalkens, A. Burbanks, and S. Wiggins, *J. Chem. Phys.* **121**, 6207 (2004).
 - [6] W. H. Miller, *J. Phys. Chem. A* **102**, 793 (1998).
 - [7] R. S. Friedman and D. G. Truhlar, *Chem. Phys. Lett.* **183**, 539 (1991); T. Seideman and W. H. Miller, *J. Chem. Phys.* **95**, 1768 (1991).
 - [8] R. Hernandez and W. H. Miller, *Chem. Phys. Lett.* **214**, 129 (1993); R. Hernandez, *J. Chem. Phys.* **101**, 9534 (1994).
 - [9] L. E. Fried and G. S. Ezra, *J. Chem. Phys.* **92**, 3144 (1988); P. Crehan, *J. Phys. A* **23**, 5815 (1990).
 - [10] Y. Colin de Verdière and B. Parisse, *Comm. PDE* **19**, 1535 (1994); *Ann. Inst. Henri Poincaré (Physique Théorique)* **61**, 347 (1994); *Comm. Math. Phys.* **205**, 459 (1999).
 - [11] S. Nonnenmacher and A. Voros, *J. Phys. A:Math. Gen.* **30**, 295 (1997).
 - [12] C. Eckart, *Phys. Rev.* **35**, 1303 (1930).
 - [13] N. Moiseyev, *Phys. Rep.* **302**, 211 (1998); W. P. Reinhardt, *Ann. Rev. Phys. Chem.* **33**, 223 (1982); B. Simon, *Phys. Lett. A* **71**, 211 (1979).
 - [14] A. Neumaier and V. A. Mandelshtam, *Phys. Rev. Lett.*

- 86**, 5031 (2001). (2005)
- [15] S. C. Creagh, Nonlinearity **17**, 1261 (2004); *ibid.* **18**, 2089